ADVANCED FUNCTIONAL MATERIALS

Supporting Information

for

Advanced Functional Materials, adfm.200600902

Bidirectional Ring-Opening and Ring-Closing of Cationic 1,2-Dithienylcyclopentenes Molecular Switches Triggered with Light or Electricity

Brian Gorodetsky and Neil R. Branda*

Department of Chemistry, Simon Fraser University, 8888 University Drive, Burnaby, BC, Canada V5A 1S6

SUPPORTING INFORMATION

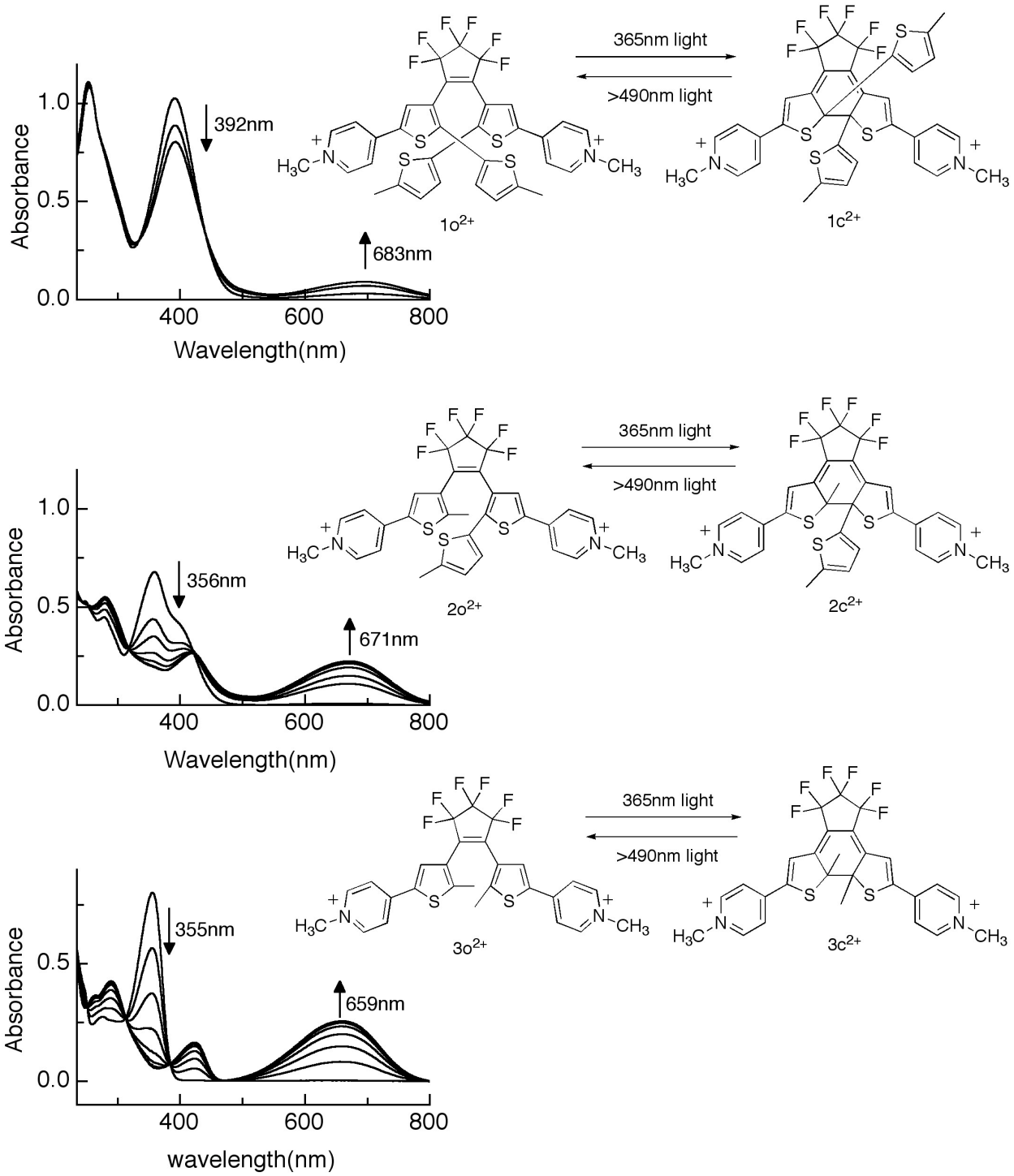

Figure S1. Photochemical ring-closing reactions of solutions of $\mathbf{1o}^{2+}$ (top, 2×10^{-5} M), $\mathbf{2o}^{2+}$ (middle, 1.8×10^{-5} M) and $\mathbf{3o}^{2+}$ (bottom, 1.5×10^{-5} M) in CH_3CN using a 365-nm light source and monitored by UV-vis absorption spectroscopy. Photoconversions to the ring-closed isomers are marked with an increase in the visible absorption bands and a decrease in the UV absorption bands.

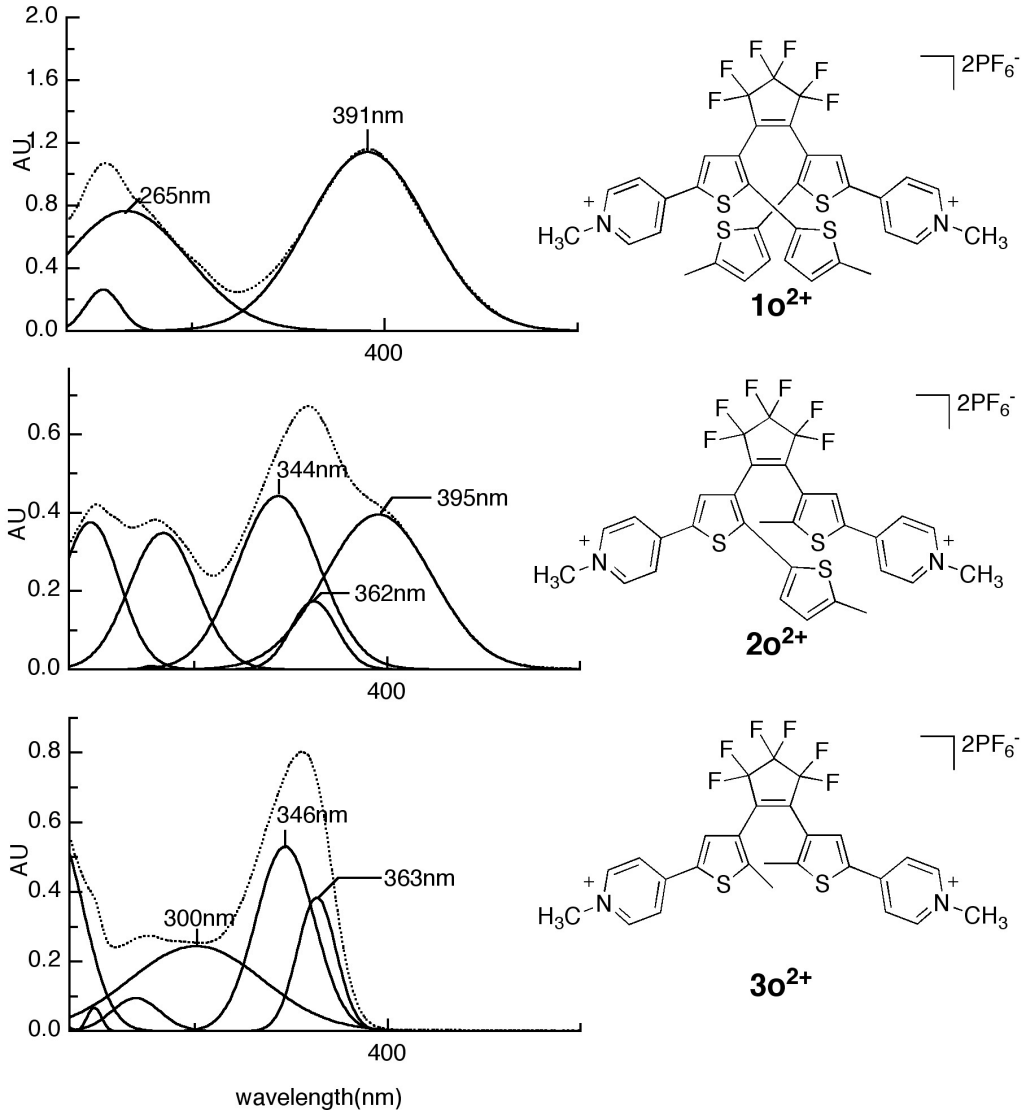

Figure S2. Comparison of the deconvoluted UV-vis absorption spectra of the ring-open isomers of the bis(pyridinium) DTE derivatives $\mathbf{1o}^{2+}$, $\mathbf{2o}^{2+}$ and $\mathbf{3o}^{2+}$ obtained using Peakfit™ simulation software. The dotted line is the overlapped observed and calculated spectrum resulting from a sum of the resolved electronic transitions (solid lines). Observed and calculated fits were statistically significant with r^2 values > 0.9999.

Spontaneous, non-photochemical ring-opening reactions. The spontaneous ring-opening reactions of the ground states of $\mathbf{1c}^{2+}$, $\mathbf{2c}^{2+}$, $\mathbf{3c}^{2+}$ and their corresponding acidified non-alkylated pyridine precursors (**8c**, **9c**, **10c**) were followed by UV-vis absorption spectroscopy at four different temperatures as summarized in Figure 4 in the manuscript. Stock solutions (1×10^{-4} M) of each of the ring-open derivatives were prepared in anhydrous and deoxygenated CH_3CN. These stock solutions were used to prepare samples of each of the compounds (1 mL) in quartz cuvettes (1 cm path-length). The samples were irradiated with UV light at room temperature (365 nm light for the alkylated pyridinium series and 313 nm for the non-alkylated pyridine series) and the photo-conversions to the ring-closed isomers were monitored by UV-vis absorption spectroscopy. The samples were irradiated with appropriate time periods to afford 3 different amounts of the ring-closed isomers (approximately 50%, 75% and 100%) to provide an internal standard for first-order kinetics behavior. To these solutions was then added 50 μL of TFA for the dual purpose of acidifying the bis(pyridine) series and to maintain constant solvent polarity and ionic strength between all samples for kinetic comparison. The prepared samples were then inserted into a Peltier temperature regulated UV-vis multi-cell chamber and were allowed to equilibrate to the experimental temperature for 3 min prior to commencing the experiments. Spontaneous ring-opening was marked by a decrease in the maximal visible absorption wavelengths, which were recorded as a function of time using 1 min intervals. The specific rate constants were then obtained by plotting $\ln(A_o/A_i)$ vs. time (first-order approximation) which provided rate-constants that were insensitive to starting concentration (typical of first-order reactions). These rate constants were then used to construct Arrhenius and Eyring plots to generate the thermodynamic data reported in Table 2 in the manuscript. The thermal ring-opening reactions were also confirmed separately using ^{1}H NMR spectroscopy to ensure that the decolourization was not due to acid-catalyzed degradation.

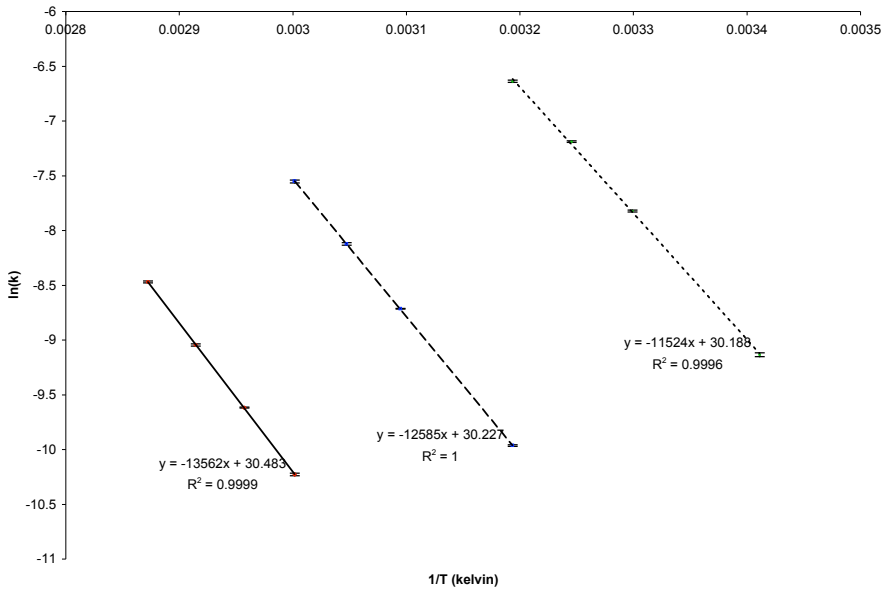

Figure S3. Comparative Arrhenius plots for the spontaneous, non-photochemical ring-opening reactions of $\mathbf{1c}^{2+}$ (dotted line), $\mathbf{2c}^{2+}$ (hashed line), $\mathbf{3c}^{2+}$ (solid line) in 5% TFA/CH_3CN.

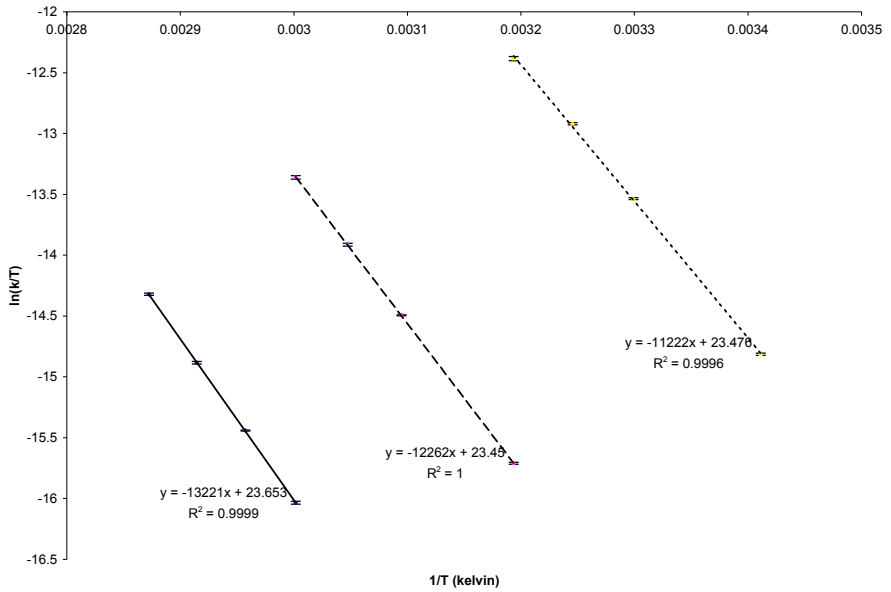

Figure S4. Comparative Eyring plots for the spontaneous, non-photochemical ring-opening reactions of $\mathbf{1c}^{2+}$ (dotted line), $\mathbf{2c}^{2+}$ (hashed line), $\mathbf{3c}^{2+}$ (solid line) in 5% TFA/CH_3CN.

^{1}H NMR spectroscopy to monitor electrolytic conversions of $\mathbf{1o}^{2+}$, $\mathbf{2o}^{2+}$, and $\mathbf{3o}^{2+}$. Approximately 2 mL of 2×10^{-3} M solutions of each of the ring-open DTE derivatives were prepared in CD_3CN/0.1 M TBAP in a glove box equipped with electrochemical feed-through leads. The solutions were reduced at –1.0 V vs. SCE using a PINE AFCBP1 bipotentiostat for 10 min (average current was 1–0.5 mA) using a platinum coil working electrode, platinum coil counter electrode and silver-wire quasi-reference electrode. Each electrode compartment was separated from each other by glass filter. Once complete, the deep blue-green solutions were removed from the working cell and added to a vial containing $AgPF_6$ (20 mg, excess). The vial was sealed and incubated at 0 ºC for 30 min to oxidize the initially produced radical-cations. The solutions were then filtered through Celite to remove the silver precipitate, providing translucent blue-green solutions that were directly transferred to NMR tubes. The ^{1}H NMR spectra were subsequently recorded on a Bruker 600 MHz spectrometer that was pre-cooled to 5 ºC. After the spectra were acquired, the solutions were transferred back into the glove box and oxidized for 10 min using 1500 mV vs. SCE potentials (average current 0.5–0.2 mA) at room temperature. The decolourized solutions are then transferred to fresh NMR tubes and the NMR spectra subsequently recorded.

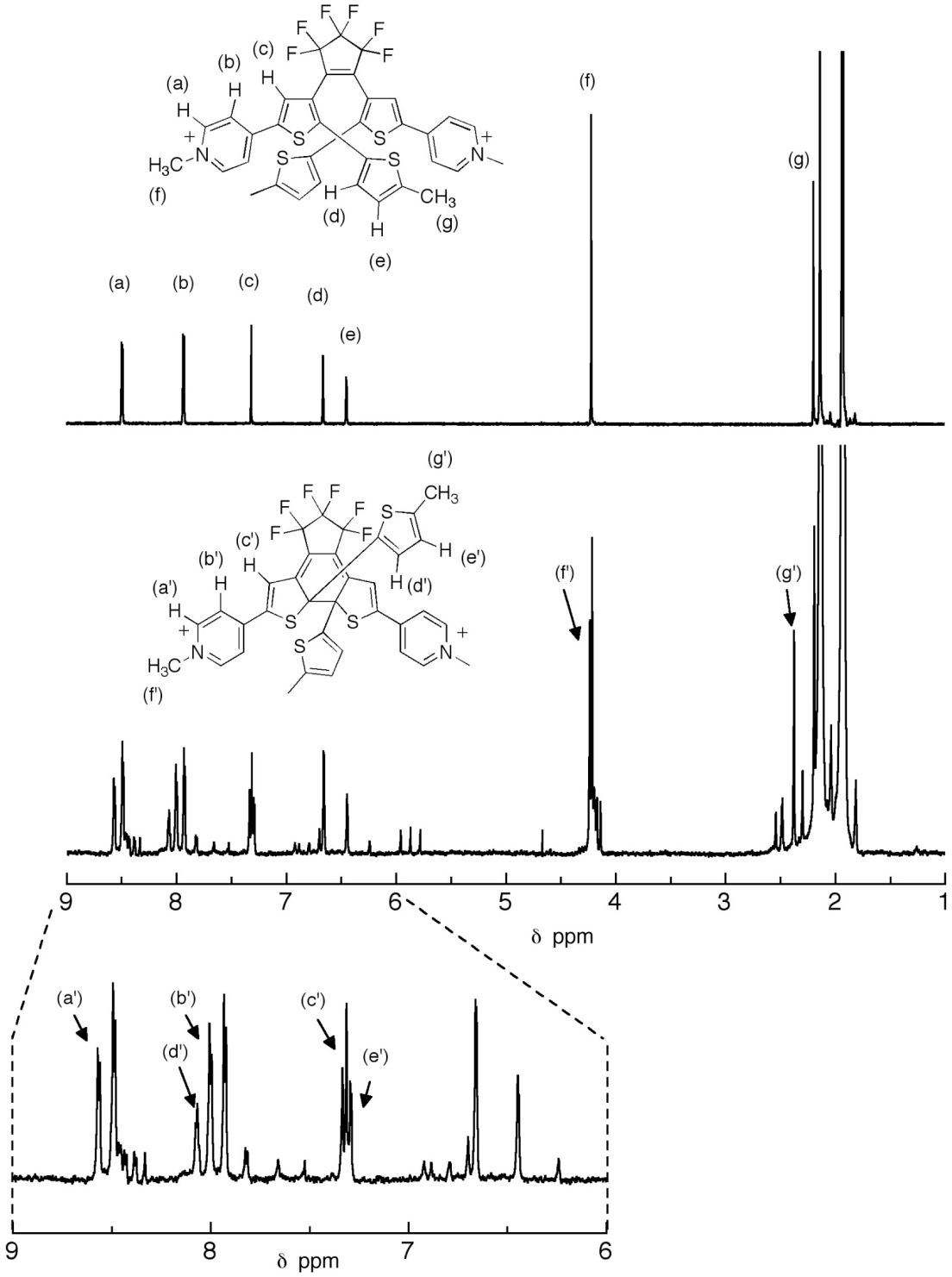

Figure S5. 600 MHz ^{1}H NMR spectra of a CD_3CN solution of **1o**$^{2+}$ (top) and the photostationary state generated by irradiating the solution with 365-nm light (bottom) showing the formation of side products.

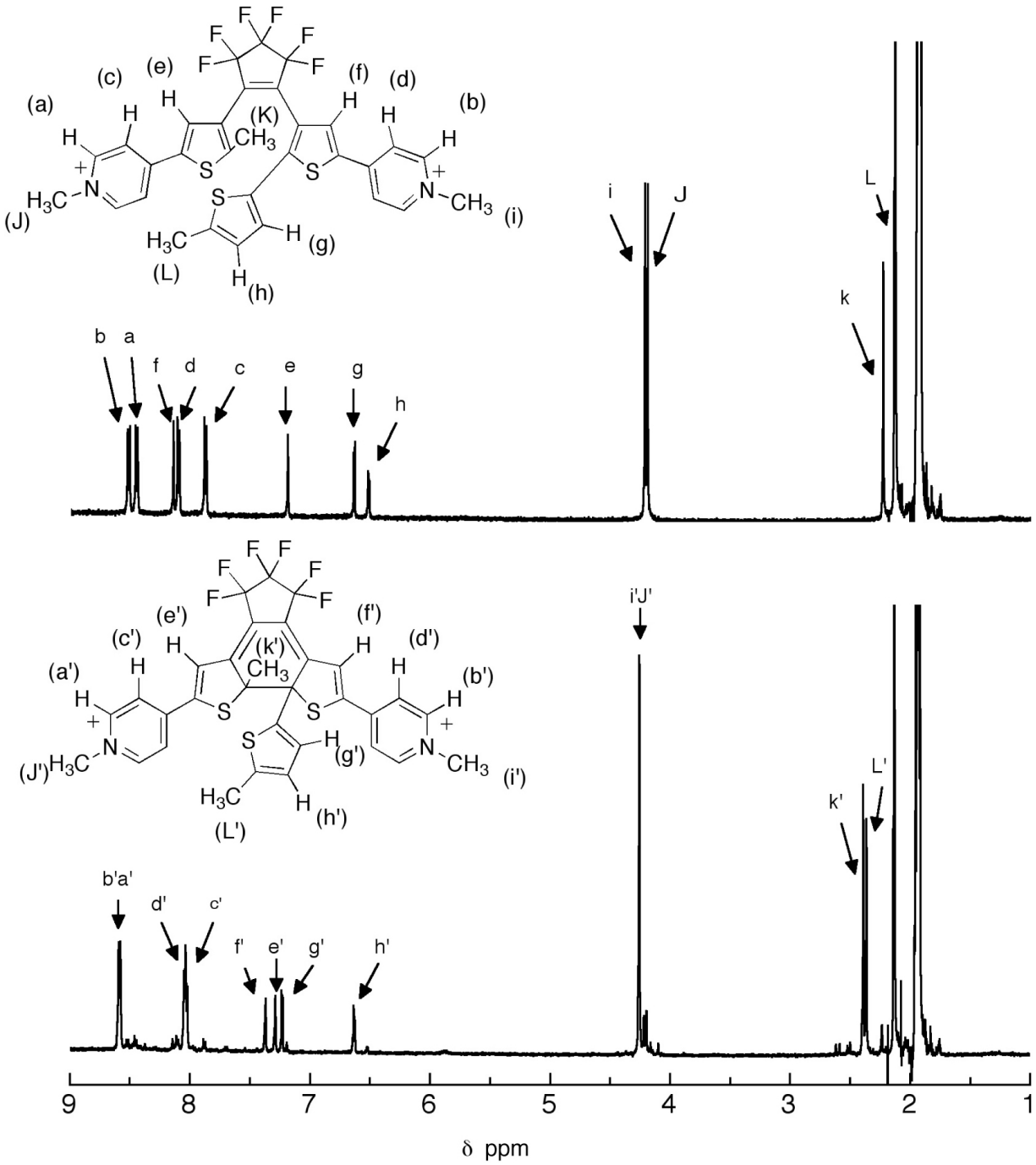

Figure S6. 400 MHz ^{1}H NMR spectra of a CD_3CN solution of **2o**$^{2+}$ (top) and the photostationary state generated by irradiating the solution with 365-nm light (bottom).

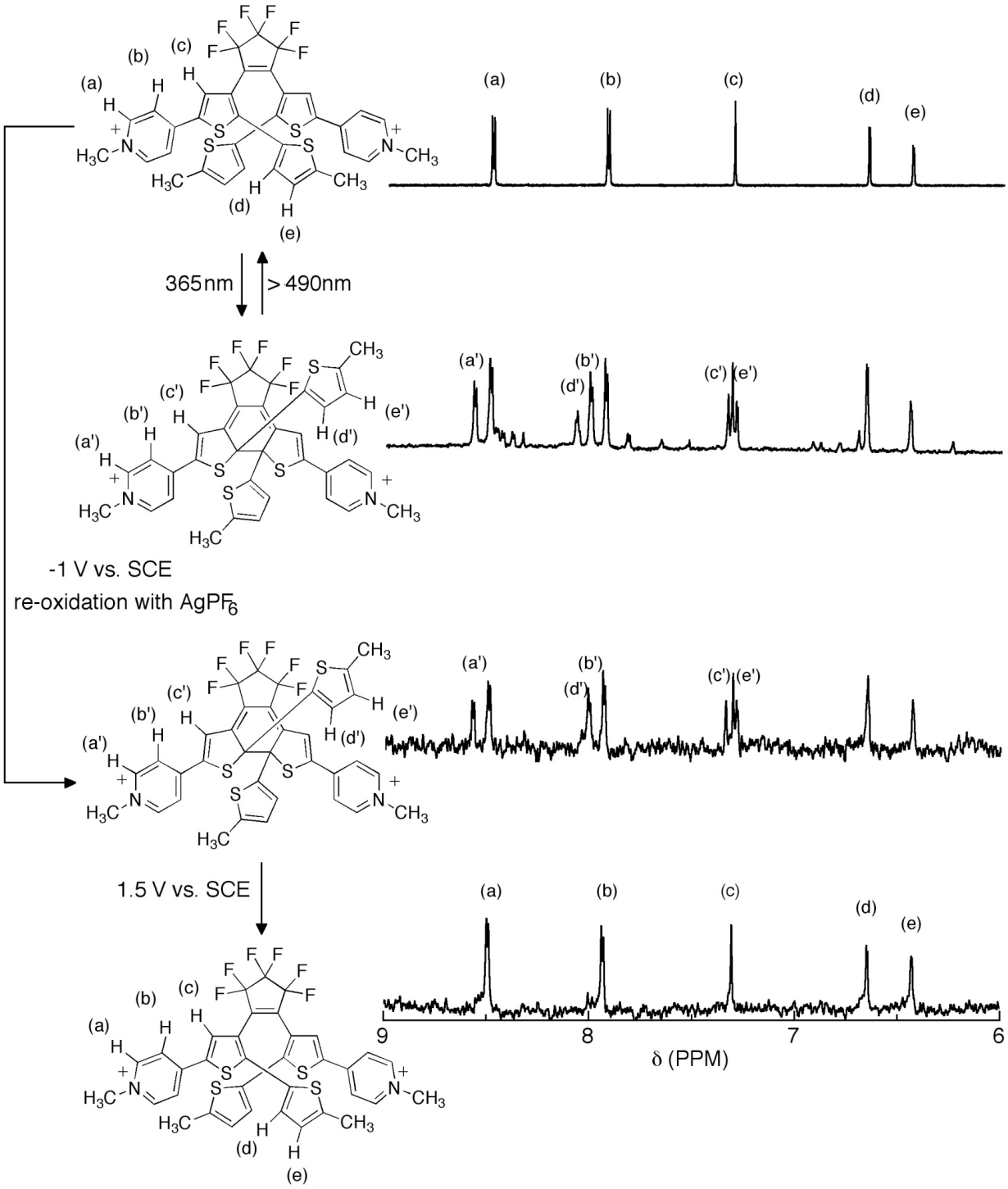

Figure S7. Selected regions of the ^{1}H NMR (600 MHz) spectra of the photochemically and electrochemically reacted DTE **1o**$^{2+}$ (1 mg/ml in CD_3CN/0.1 M TBAP). The radical initially produced by the reductive ring-closing was quenched by the addition of $AgPF_6$ and the solution was maintained at 0 ºC to minimize spontaneous ring-opening.

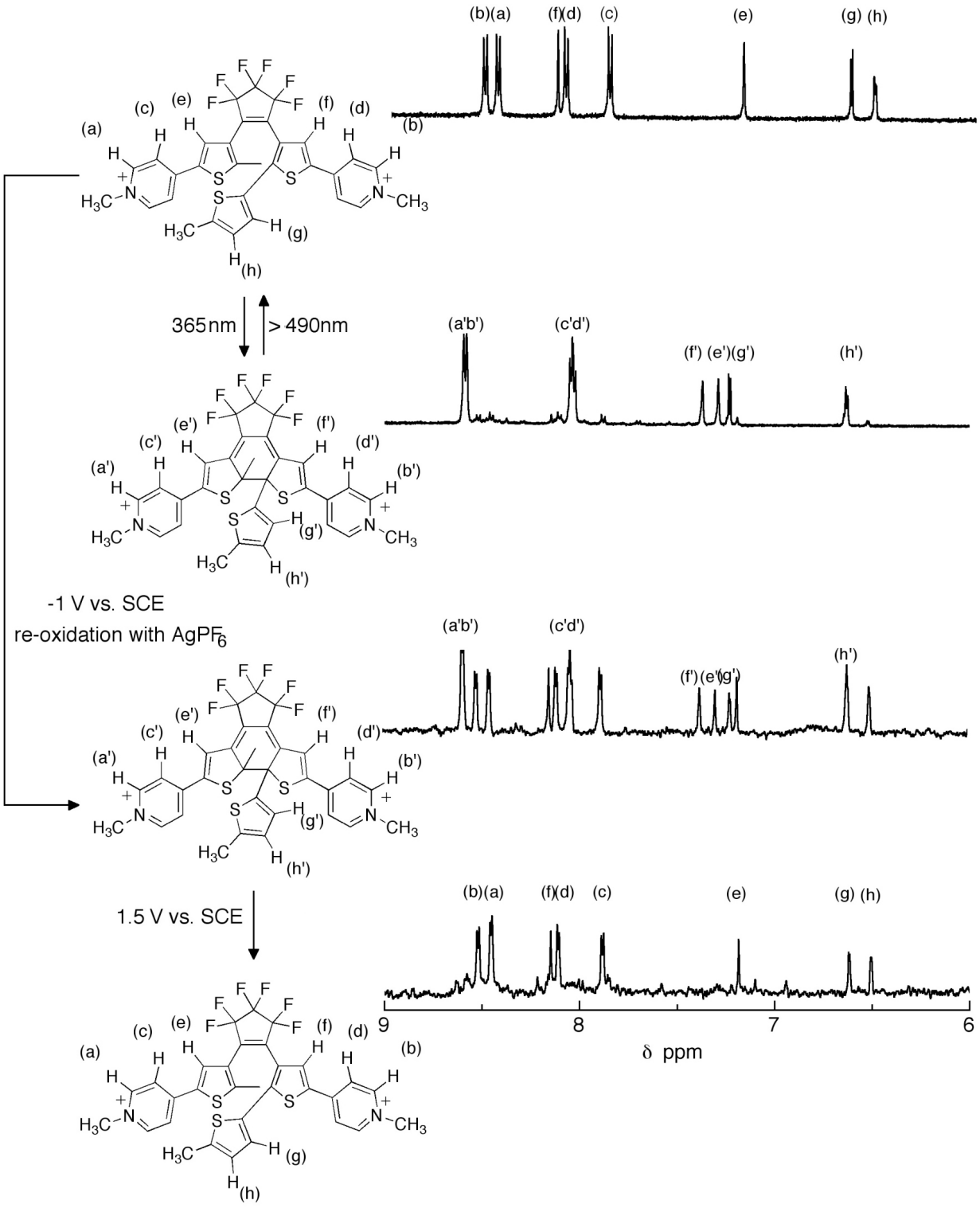

Figure S8. Selected regions of the ^{1}H NMR (600 MHz) spectra of the photochemically and electrochemically reacted DTE **2o**$^{2+}$ (1 mg/ml in CD_3CN/0.1 M TBAP). The radical initially produced by the reductive ring-closing was quenched by the addition of $AgPF_6$ and the solution was maintained at 0 ºC to minimize spontaneous ring-opening.

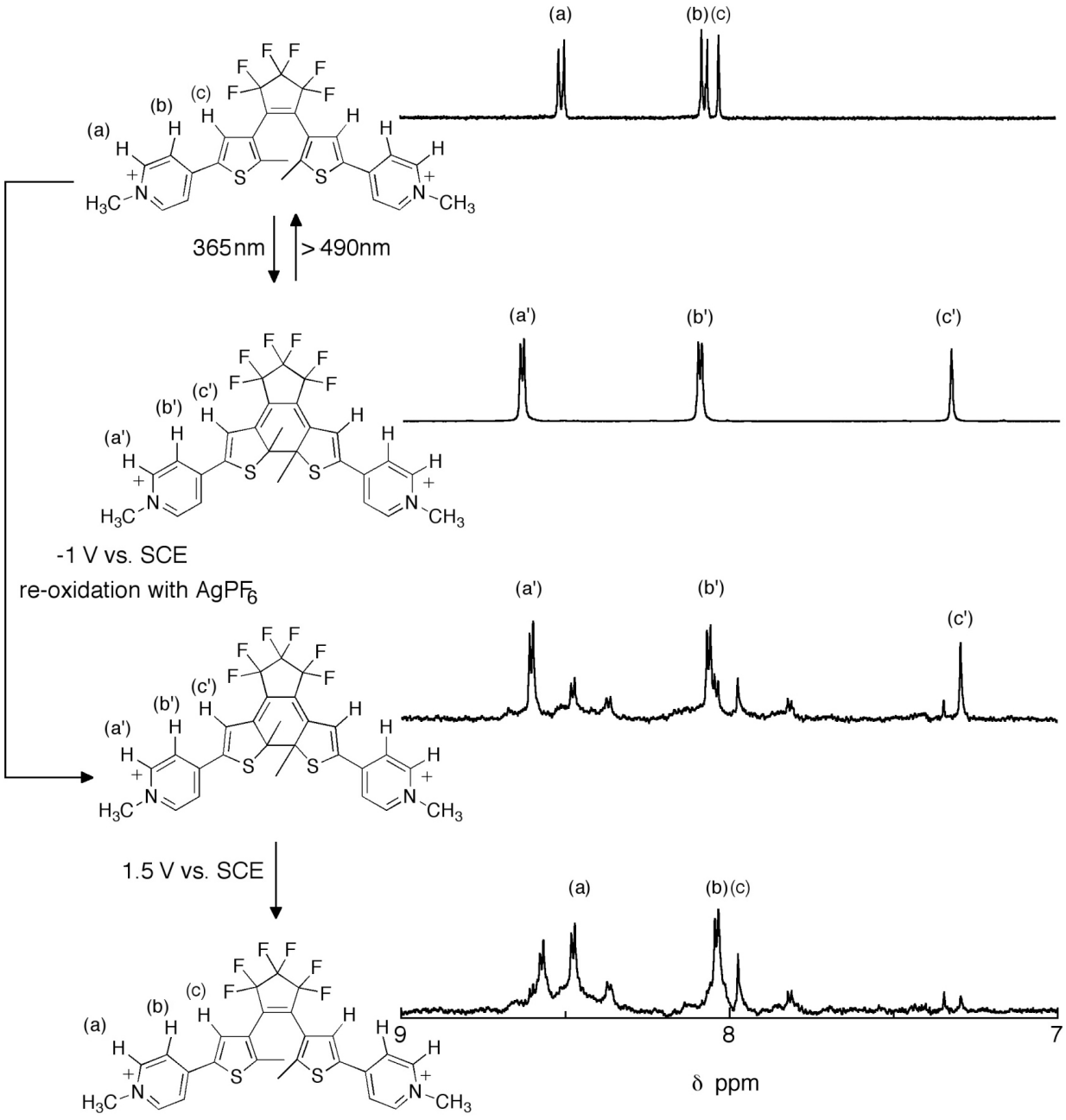

Figure S9. Selected regions of the ^{1}H NMR (600 MHz) spectra of the photochemically and electrochemically reacted DTE **3o**$^{2+}$ (1 mg/ml in CD_3CN/0.1 M TBAP). The radical initially produced by the reductive ring-closing was quenched by the addition of $AgPF_6$ and the solution was maintained at 0 ºC to minimize spontaneous ring-opening.

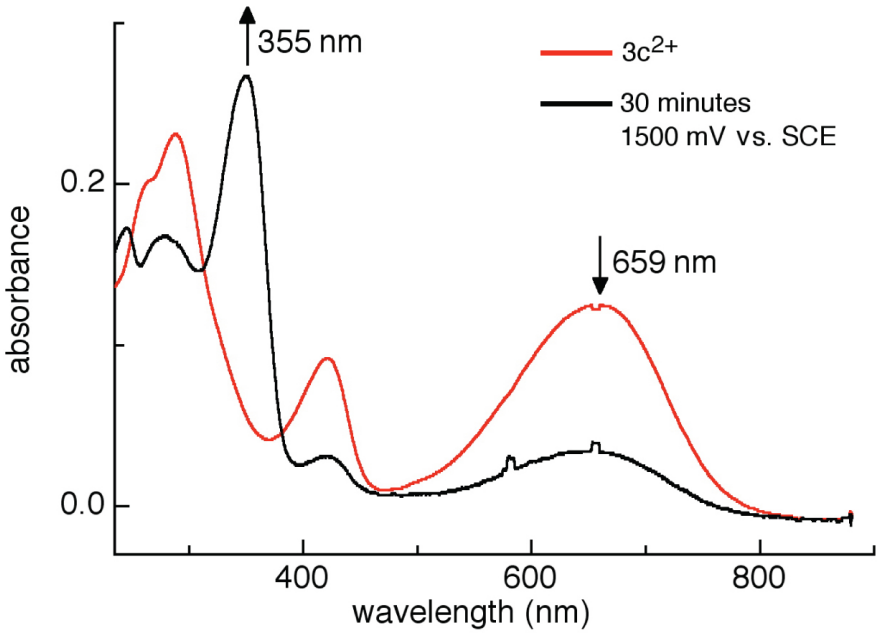

Figure S10. Changes in the UV-vis absorption spectra when solutions of **3c**$^{2+}$ (2×10^{-4} M in CH_3CN/0.1 M TBAP) are subjected to electrochemical oxidation. The changes correspond to those typical of the ring-opening reaction.